Novel Third Harmonic Current Injection Technique for Harmonic Reduction of Controlled Converters

Ali M. Eltamaly[†]

[†]Sustainable Energy Technologies Center, Dept. of Electrical Eng., King Saud University, Riyadh, Saudi Arabia

Abstract

Three-phase controlled converters have many applications in the utility interfacing of renewable energy sources and adjustable speed drives as a rectifier or inverter. The utility line currents of these converters have a high harmonic distortion, which is more than the harmonic standards. This paper introduces a new technique for circulating the third harmonic currents from the dc-link to the line currents to reduce their harmonic contents. The proposed system uses a single-phase PWM converter to control the angle and amplitude of the injection current for each of the firing angle of a three-phase converter. A detailed analysis is introduced to achieve a relationship between the firing angle of the three-phase controlled converter and the power angle of the PWM converter. In addition, a detailed design for the other injection path components is introduced. A simulation and experimental work is introduced to prove the mathematical derivations. Analysis, simulation and experimental results prove the superiority of the proposed technique.

Key words: Harmonic distortion, Three-phase controlled converter, third harmonic injection, power quality

NOMENCLATURE

I_f	The third harmonic injection current.
v_a, i_a	The voltage and current of phase a.
α	The firing angle of the three-phase converter.
θ_{on}	The angle of $V_{on,3}$ referred to v_a in the 180 Hz domain.
Ψ	The angle between $V_{on,3}$, and I_f in the 180 Hz domain.
Ψ_{opt}	The angle between $V_{on,3}$, and I_f for the minimum THD in the line currents in the 180 Hz domain.
Φ	The angle between V_a and I_f in the 180 Hz domain.
Φ_{opt}	The angle between V_a, and I_f for the minimum THD in the line currents in the 180 Hz domain.
V_m	The peak value of the phase voltage.
ω	The angular velocity of the fundamental frequency.
V_{LL}	The rms value of the line to line supply voltage.
V_{dn}	The rms value of the voltage between points d and n.
V_{fn}	The rms value of the voltage between points f and n.
$V_{on,3k}$	The rms value of the $(3k)$ harmonic of the voltage between points o and n.
k	$=1, 2 , 3, 4, ...$
a_0, a_h, b_h	Fourier coefficients.

L_{dc} , C_{dc}	Inductor and capacitor in the dc-link.
m_a	Modulation index of the single-phase PWM converter.
δ	Power angle of the single-phase PWM converter.
X_{odf}	Reactance between "o" and "d" or between "o" and "f".

I. INTRODUCTION

Three-phase controlled converters have many applications such as ac and dc adjustable speed drives (ASD) [1]-[5], induction heating, HVDC power systems, power supplies and utility interfacing of renewable energy (RE) systems with electric utilities [6]-[10]. These applications use controlled converters as a rectifier or as an inverter. The line currents of controlled converters have high harmonic contents with respect to PWM converters that use IGBT. However, apart from the higher switching losses associated with PWM converters, the power handling capability and reliability of these devices are quite low when compared to SCRs [10]. Moreover, some applications especially in high ratings prefer line commutated converters over PWM due to the high EMI associated with PWM. Many techniques have been introduced to reduce these harmonics such as a reduction by using increased pulse numbers, IPN [11], active and passive filters, APF [12]-[14], modulation of the controlled signal of
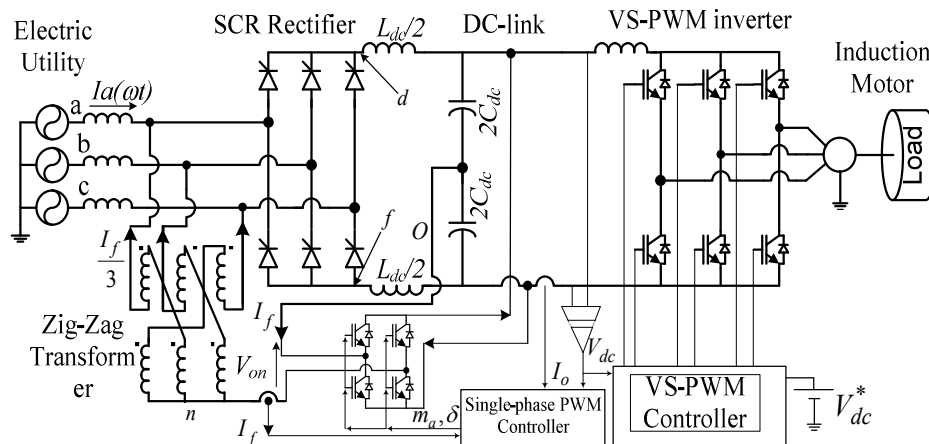
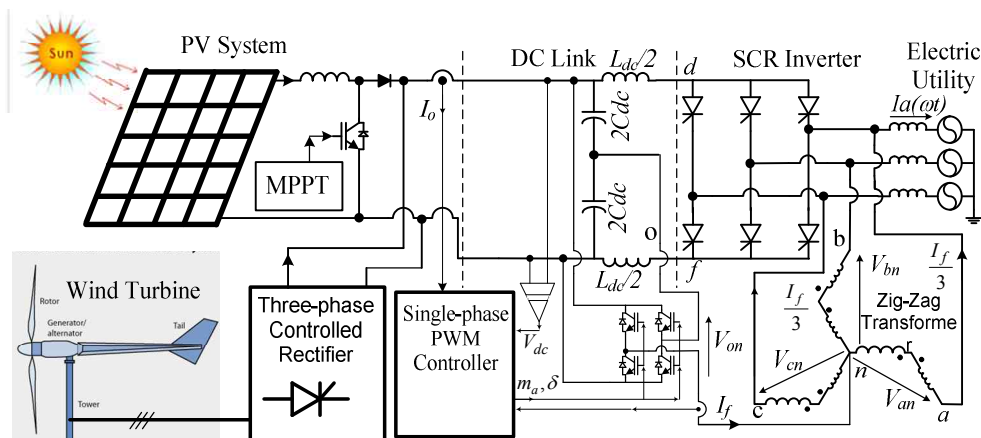Fig. 1. The proposed approach as a rectifier in ASD.

Fig. 2. The proposed approach as an inverter in renewable energy applications.

dc-dc converters connected to a converter by third harmonic components, MCC [15], or by third harmonic injection from the dc-link to the line currents, 3rd_INJ [16]–[19]. The third harmonic injection technique was used in uncontrolled converters in [20]–[23]. A review of the three-phase improved power quality of uncontrolled converters by different techniques is shown in [24]. The third harmonic injection technique in a controlled converter was first introduced in 1969 [25]. This technique uses the third harmonic voltage in the dc-link to inject a current to the line currents. References [26] and [27] used the three LC branches tuned around triple the utility frequency to inject the third harmonic current into the line currents. This technique has many disadvantages due to its high cost, the fact that it is bulky, and its need of precise values for L and C to share the third harmonic currents equally. References [28], [29] used an interfacing delta-star transformer to circulate the injection current to the neutral of the star. This technique increases the cost due to the interfacing transformer. Other references [18], [19] used star-delta transformer in the reinjection path with an unloaded delta to circulate the injection current through the neutral of the star to the line currents. Some other

references [16], [20], [30], and [31] used a partial rating (20%) zigzag transformer to circulate the third harmonic injection current to the line currents to replace the need for a full load Δ/Y transformer. The injection of the third harmonic has been controlled by using a single-phase boost rectifier to circulate the power in the third harmonic path back to the dc-link to increase the converter efficiency [31]. This technique is suitable for uncontrolled rectifiers because it is easy to control the third harmonic current in the injection path, but it cannot control the angle of the injection current that should be changed with changing the firing angle of the three-phase controlled converter [31], [32]. The new proposed technique introduced in this paper avoided this limitation by controlling the phase angle and amplitude of the injection current by controlling the power angle and modulation index of the single-phase PWM converter, respectively, in the injection path. This is shown in Fig. 1 and Fig. 2 for the ASD and the RE, respectively. Therefore, the main contribution of the proposed technique in this paper is the decoupling between the amplitude and the angle of the injection current which has not been introduced before. Reference [30] used a bidirectional switch in the third

TABLE I

A COMPARISON BETWEEN THE CONVENTIONAL HARMONIC
REDUCTION AND THE PROPOSED TECHNIQUES

Technique	CUC*	ROI*	ACC*	3rd AC*	ITC*
IPN [12]	Diode Only	Rec. Only	Yes	NA	Complex
APF [12]-[14]	Both	Both	Yes	NA	No need
MCC [15]	Diode Only	Rec. only	Yes	NA	No need
LC branches [26], [27]	Both	Both	Yes	Yes	No need
3rd_INJ [18],[19]	Both	Rec. only	Yes	No	Y/unloaded Δ
3rd_INJ [28, 29]	Both	Rec. only	Yes	No	Δ/Y
3rd_INJ[16], [20], and [30]	Both	Rec. only	Yes	No	Zig-zag
3rd_INJ [31]	Both	Both	Yes	No	Zig-zag
Proposed	Both	Both	Yes	Yes	Zig-zag
IGBT	NA	Both	NA	NA	No need

*CUC= Controlled or uncontrolled Converters.
*ROI = Rectifier or inverter
*ACC= Amplitude of third harmonic current control.
*3rd AC = Third Harmonic Angle Control.
*ITC=Interface Transformer.

harmonic injection path to control the injection current for each firing angle of the controlled converter. However, this technique has a limitation since controlling the injection current angle affects its amplitude and vice versa. This limitation has been avoided in the proposed technique by decoupling between the amplitude and the angle of the injection current. The power angle of the single-phase PWM converter, δ, is used to control the angle of the third harmonic injection current, ϕ. The modulation index, m_a, of the single-phase PWM converter is used to control the amplitude of the third harmonic current, I_f. A generalized analysis for a three-phase controlled converter with the proposed injection technique is proposed to be used in case of a rectifier or an inverter. A new mathematical derivation to get the relation between the firing angle of a three-phase controlled converter, α, and the corresponding optimum value of the power angle of a single-phase PWM converter, δ, is introduced. This is the main contribution of this paper. In addition, the design details for the single-phase PWM converter are introduced. Excellent results in harmonic reductions of the utility line currents of three-phase controlled converters have been obtained. A detailed comparison between conventional harmonic reduction techniques and the proposed technique is shown in Table I.

If the supply voltage of phase a is taken as a reference vector, $v_a(\omega t) = V_m \sin(\omega t)$ as shown in Fig. 3(a) at α=20°. Fig. 3(b) shows the injection current along with $v_a(\omega t)$. Fig. 3 (c) shows the voltage of phase a and the reinjection current. The waveforms of voltages at the dc-link, V_{dn}, V_{fn} and V_{on}, are shown in Fig. 3(d). These voltages are the voltages that were

(a) Voltage and current of phase a.

(b) Voltage of phase a and reinjection current.

(c) Voltage, current of phase a and reinjection current.
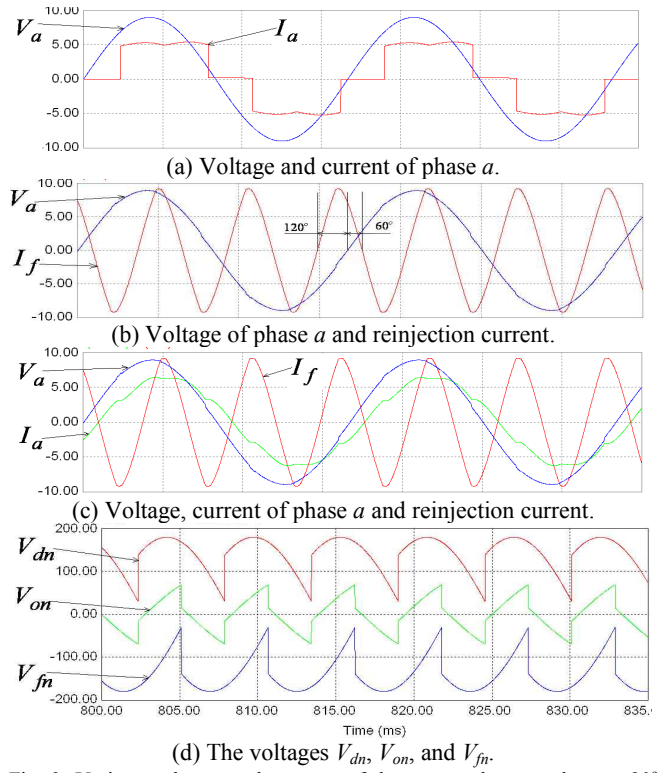
(d) The voltages V_{dn}, V_{on}, and V_{fn}.

Fig. 3. Various voltages and currents of the proposed approach at α=20° [31].

used to circulate the third harmonic current in the injection path. Therefore, by using the complex Fourier analysis for these voltages, the relation between the voltage, $V_{on,3k}$, and angle α can be obtained from the following equations:

$$V_{on,3k} = \frac{3V_{LL}}{\pi(9k^2 - 1)}\sqrt{1 + (9k^2 - 1)\sin^2 \alpha} \qquad (1)$$

And angle of $V_{on,3k}$ for *odd values of k* is,

$$\theta_{on,3k} = \tan^{-1}\left[\frac{k_n \sin(k_p \alpha) - k_p \sin(k_n \alpha)}{k_p \cos(k_n \alpha) - k_n \cos(k_p \alpha)}\right] \qquad (2)$$

$V_{on,3k}$ = 0 for even values of k
where:

$$k_n = 3k - 1 \quad \text{and} \quad k_p = 3k + 1. \qquad (3)$$

Fig. 4 shows the FFT components of $V_{on,3k}$ at α=40°. It is clear from Fig. 4 that the third harmonic voltage $V_{on,3}$ is the most dominant component in $V_{on,3k}$. Therefore, tuning the harmonic injection path around triple the utility frequency will circulate the third harmonic current freely. As a result, the following analysis will focus on the third harmonic component. By substituting k =1 in (1) and (2), the voltage, $V_{on,3}$, and its angle can be obtained as shown in (4) and (5), respectively [31], [32].
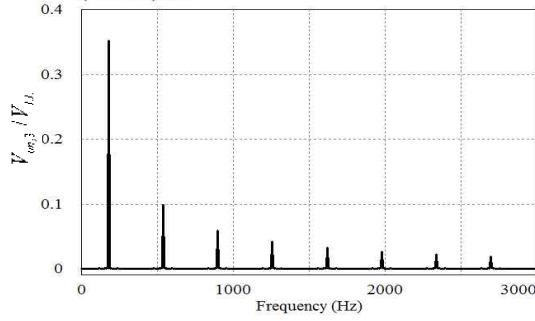
Fig. 4. FFT components of V_{on} at $\alpha=40^o$.
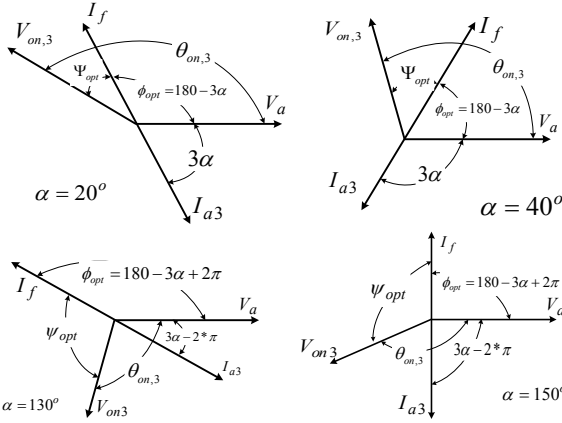
Fig. 5. Phase difference between components for, $\alpha=20^o$, 40°, 130° and 150° respectively.
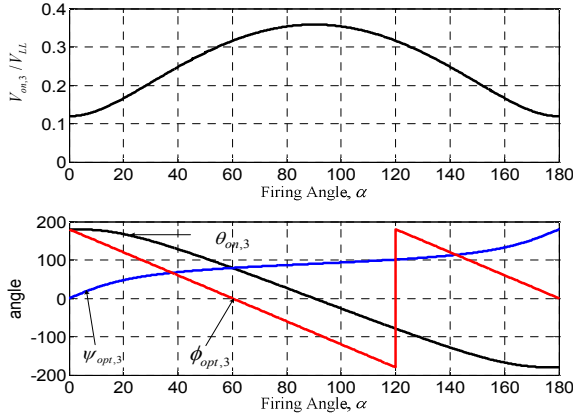
Fig. 6. The variation of V_{on3}/V_{LL}, $\theta_{on,3}$, $\theta_{opt.3}$, $\psi_{opt,3}$ along with α.

$$V_{on,3} = \frac{3V_{LL}}{8\pi}\sqrt{1+8\sin^2\alpha} \tag{4}$$

$$\theta_{on,3} = \tan^{-1}\left[\frac{\sin(4\alpha)-2\sin(2\alpha)}{2\cos(2\alpha)-\cos(4\alpha)}\right] \tag{5}$$

The optimum angle between the third harmonic component of the injection current, I_{f3}, and supply current of phase a with respect to 180 Hz, I_{a3}, is 180° [20], [31] and [32]. Depending on this logic, the injection current, I_{f3}, can be drawn with respect to I_{a3} at the optimum injection angle. As shown in Fig. 3, the voltage, v_a, has been taken as a reference.

Therefore, the phase angle of the fundamental current of the phase a current is $-\alpha$ and -3α with respect to the utility and triple the utility frequencies, respectively. Then the optimum angle, ϕ_{opt}, between v_a and I_{f3} is shown in (6).

$$(\phi_{opt}) = 180 - 3\alpha \tag{6}$$

In addition, the optimum angle between $V_{on,3}$ and I_{f3} is ψ_{opt}, which can be obtained from the following equation:

$$\psi_{opt} = \theta_{on,3} + 3\alpha - 180 \tag{7}$$

From (6) and (7) the phase angle between each of the vectors for various firing angles; $\alpha=20^o$ and 40° (as an example for the rectifier mode) and $\alpha=130^o$ and 150° (as an example for the inverter mode) are shown in Fig. 5. From (4) the relation between $V_{on,3}/V_{LL}$ and the firing angle, α, is shown in Fig. 6. In the same way, from (6) and (7), the variation of $\theta_{on,3}$, ϕ_{opt}, and ψ_{opt} along with the firing angle of the three-phase converter, α, are shown in Fig. 6.

II. THE OPTIMUM AMPLITUDE OF INJECTION CURRENT

The amplitude of the optimum injection current for minimum THD, is a function of the dc-link current, I_o. Therefore, the amplitude of the injected current can be assumed to be qI_o where q is a proportional constant. Then the equation of the injected current, i_{f3}, can be obtained from the following equation:

$$i_{f3} = -\frac{q}{3}I_o \sin(3(\omega t - \alpha)) \tag{8}$$

In the case of the phase a voltage, v_a is the reference voltage. Then the current of phase a can be determined from the following equation:

$$i_a(\omega t) = \begin{cases} I_o + \dfrac{i_f}{6} = I_o - \dfrac{q}{6}I_o \sin(3(\omega t - \alpha)) & \dfrac{\pi}{6} < \omega t - \alpha < \dfrac{5\pi}{6} \\ -I_o - \dfrac{q}{6}I_o \sin(3(\omega t - \alpha)) & \dfrac{7\pi}{6} < \omega t - \alpha < \dfrac{11\pi}{6} \\ -\dfrac{i_f}{3} = \dfrac{q}{3}I_o \sin(3(\omega t - \alpha)) & For Elsewhere \end{cases} \tag{9}$$

The rms value of the supply current, $I_{a,rms}$, can be obtained as shown in (10).

$$I_{a,rms} = \frac{I_o}{6}\sqrt{q^2 + 24} \tag{10}$$

In addition, the rms value of the fundamental component of the supply current, $I_{a1,rms}$, can be obtained by applying the Fourier transform to Eq.(9). The result is shown in the following equation:

$$I_{a1,rms} = \frac{\sqrt{6}(q+16)I_o}{16\pi} \tag{11}$$

The THD of the supply current can be obtained from (12).

$$THD = \sqrt{\frac{I_{a,rms}^2 - I_{a1,rms}^2}{I_{a1,rms}^2}} \tag{12}$$

Substituting (10) and (11) into (12) the following equation can be obtained:

$$THD = \sqrt{\frac{32\pi^2}{27}\left(\frac{q^2+24}{(q+16)^2}\right) - 1} \tag{13}$$

For the minimum THD, the derivative of the THD should be equal to zero.

$$\frac{d}{dq}THD = 0 \tag{14}$$

By substituting (13) into (14) the optimum value of q is:

$$q_{opt} = 1.5 \tag{15}$$

The value of q_{opt} is exactly the same as the value obtained for the diode rectifier [16], [33]. The theoretical minimum THD associated with this technique can be obtained from substituting (15) into (13). Then the minimum THD that can be obtained from the third harmonic injection technique is 5.12%. The optimum value of the reinjection current can be obtained from (6) and (15) and is shown in (16).

$$I_{f3} = -\frac{3}{2}I_o \sin(3\omega t - 3\alpha) \tag{16}$$

In the case of $q=1.5$ and the variable reinjection current angle, (9) can be modified to be as shown in (17).

$$i_a(\omega t) = \begin{cases} I_o + \dfrac{i_f}{6} = I_o + \dfrac{1}{4}I_o \sin(3\omega t + \phi) & \dfrac{\pi}{6} < \omega t - \alpha < \dfrac{5\pi}{6} \\[2mm] -I_o + \dfrac{1}{4}I_o \sin(3\omega t + \phi) & \dfrac{7\pi}{6} < \omega t - \alpha < \dfrac{11\pi}{6} \\[2mm] -\dfrac{i_f}{3} = -\dfrac{1}{2}I_o \sin(3\omega t + \phi) & For Else \; where \end{cases} \tag{17}$$

The rms value of the supply current, $I_{a,rms}$, can be obtained from (17) and rms of the fundamental component of the line current, $I_{a,rms}$, can be obtained by the Fourier transform of the current shown in (17). Substituting the new values of $I_{a,rms}$ and $I_{a,rms}$ into (13) and equating the derivative of the THD by zero, the optimum relation between α and ϕ_{opt} can be obtained, which is the same that previously obtained in (6). The variation of the THD with the firing angle α at $q=1.5$ is shown in Fig. 7.

TABLE II

THE VALUES OF EACH COMPONENTS OF THE PROPOSED MODEL

Component	Value
kVA rating of the model	2kVA
Line Voltage	220V
L_{dc}, and C_{dc},	6.42mH, and 220μF respectively
X_{odf}	1.614 Ω
Source Inductance	0.1mH
I_o and I_f	3A and 3.182 respectively
VA rating of single-phase PWM converter	0.11*2000=220VA
VA rating of zig-zag transformer	0.202*2000=404VA

III. DESIGN EXAMPLE

A prototype model has been used to demonstrate the above analysis. The model is designed to feed 2kVA loads with a supply line voltage of 220V. The model is used in simulation and experimental work. The dc-link parameters, $X_{L,dc}$ and $X_{C,dc}$, are chosen to be 0.5 and 0.1 pu, respectively. From the nominal values of the components in the model, the base value of the supply current is 5.25A, and base impedance is Z_{base}=24.2Ω. Then $X_{L,dc}$=7.25Ω, $X_{C,dc}$=4.02Ω, L_{dc}=6.42mH, and C_{dc}=220μF. These values of L_{dc} and C_{dc} are equally divided in the dc-link as shown in Fig. 1 and Fig. 2. Then the impedances of each of the inductors and capacitors are 3.625 Ω and 2.011Ω, respectively, as shown in Fig. 8. Therefore, the resultant impedance between points "o" and "d" or between "o" and "f" =3.625-2.011=1.614Ω. The values of each of the components of the model are shown in Table II.

Values of $V_{on,3}/V_{LL}$ vary between $V_{on,3}/V_{LL}(\alpha=0)$ =0.1194pu and $V_{on,3}/V_{LL}(\alpha=90^o)$= 0.358pu. If the operating range of the firing angle, α, of the controlled converter is assumed to be between 0° and 60° for rectifier and between 120° to 170° for the inverter mode of operation, then the values of $V_{on,3}$ vary between $V_{on,3}/V_{LL}$ (α=0)= 0.1194pu and $V_{on,3}/V_{LL}$ (α=60°)=0.3158pu. If the suggested maximum possible dc current, I_o=3A=0.57pu, then from (16), the third harmonic injected current is I_f= 3.182A=0.606pu. Then the highest possible VA of a single-phase PWM converter occurs at the highest possible values of $V_{on,3}$ and I_{f3} which is 0.316*0.606/$\sqrt{3}$ =0.11 pu. Then the rating of the single-phase PWM converter is about 11% of the rated VA of the controlled converter.

The output dc voltage from the single-phase PWM should be connected to the dc link as shown in Fig. 1 and Fig. 2. The single-phase PWM converter replaced the single-phase uncontrolled converter in [31] to control the angle of the injection current. The third harmonic injection current can be controlled by varying the modulation index of the PWM
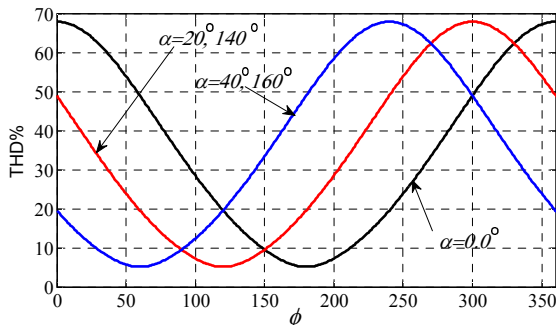
Fig. 7. The variation of THD with the angle ϕ at q=1.5 for different firing angles α.
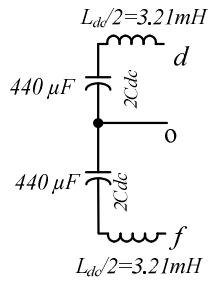

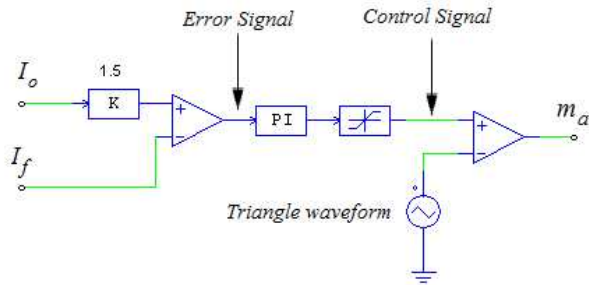Fig. 8. Tuning the third harmonic injection path around the third harmonic frequency.

Fig. 9. The schematic of the control circuit of the boost converter.
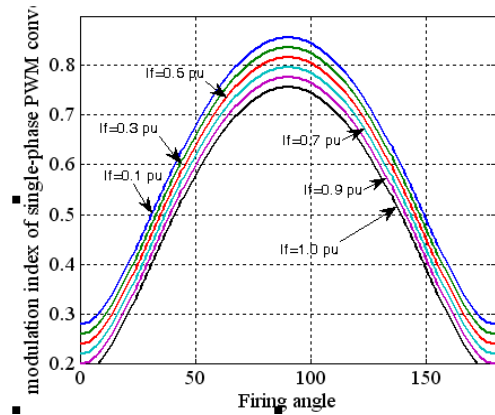

Fig. 10. The relation between the modulation index, m_a of single-phase PWM converter and firing angle of three-phase controlled converter for different values of injection current.
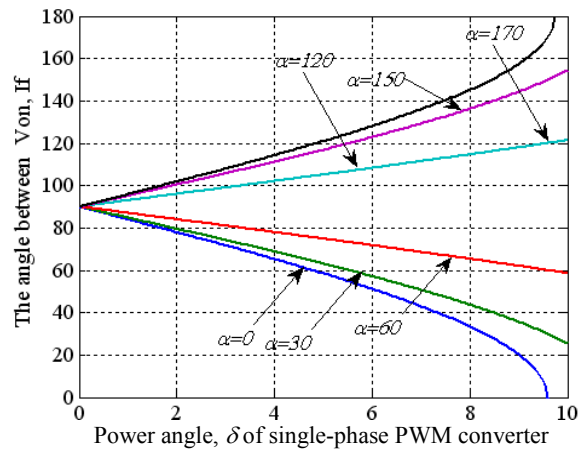

Fig. 11. The relation between angle ψ and the power angle, d of single-phase PWM converter for different values of firing angle, α.

converter. A current sensor is used to measure the actual dc-link current and the third harmonic injection current. The error signal between these two currents is used to control the modulation index, m_a, of the single-phase PWM converter. The relation between the rms value of the injected current, I_f, and the dc current, I_o, is I_f=1.5 I_o [31]. The relation between the injection current, I_f, and modulation index of the PWM converter is shown in Eq.(18). It is clear from this equation that the rms value of I_f can be easily controlled by controlling the modulation index of the single phase PWM converter. This logic has been accomplished as shown in Fig. 9. It is clear from (18) and Fig. 10 that the injection current can be controlled by controlling the modulation index, m_a, of the single-phase PWM converter.

$$ I_f = \frac{V_{on,3} - m_a V_{dc}}{X_{odf}} \tag{18} $$

The power in the 3rd harmonic injection path will return to the dc-link and can be obtained from (19) and (20). Equating

these two equations with some simplification produces the relation between the angle between $V_{on,3}$ and I_f, and ψ_{opt} and the power angle, δ, as shown in (21). It is clear from this equation that the angle ψ can be controlled by controlling the power angle, δ. The relation between ψ and the power angle, δ, for different values of the firing angle, α, is shown in Fig. 11. The output dc voltage of the single-phase PWM converter is connected to the dc-link of the three-phase controlled converter to return the power back to the dc-link.

$$ P_{3rd} = I_f V_{on,3} \cos\psi \tag{19} $$

$$ P_{3rd} = \frac{m_a V_{dc} V_{on,3}}{X_{odf}} \sin\delta \tag{20} $$

$$ \psi = \cos^{-1}\left[\frac{m_a V_{dc}}{X_{odf} I_f}\sin\delta\right] \tag{21} $$
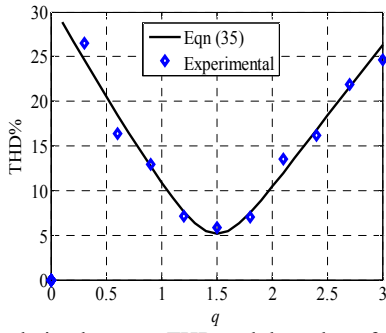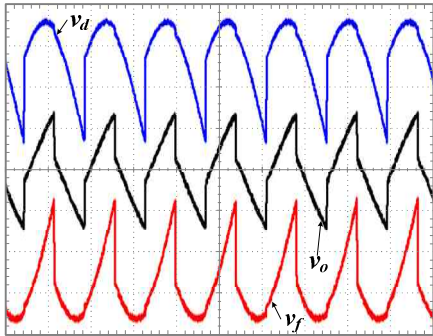
Fig. 12. The relation between THD and the value of q.

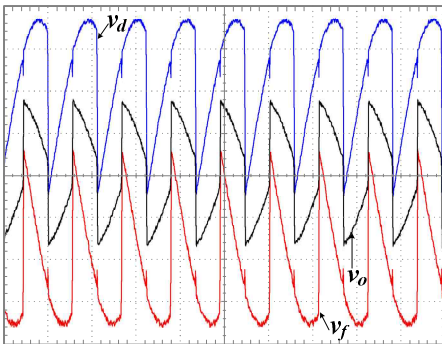Fig. 13. The voltages v_d, v_f, v_{on} at α =20° (100V/div.).

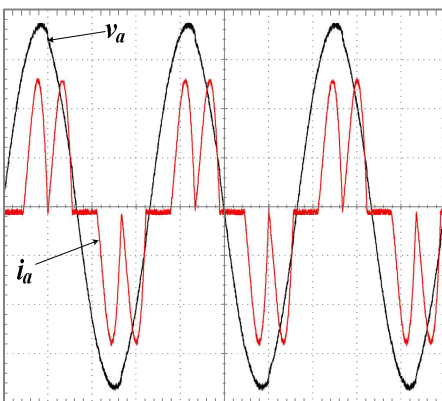Fig. 14. The voltages v_d, v_f, v_{on} at α =140° (100V/div.).

Fig. 15. The supply current along with v_a at α =20° without harmonic injection (100V/div., and 1A/div).
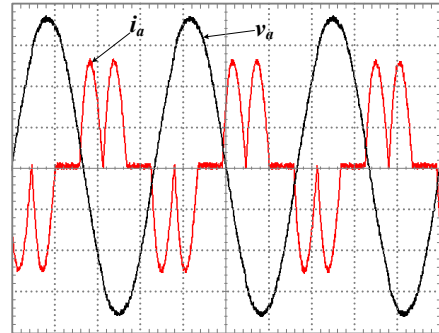

Fig. 16. The supply current along with v_a at α =140° without harmonic injection (100V/div., and 1A/div).
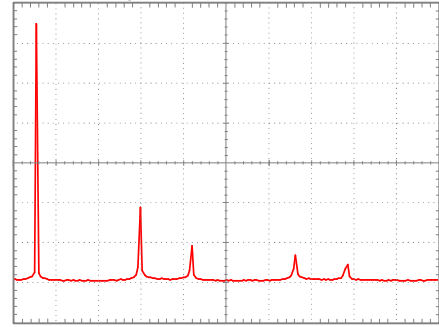

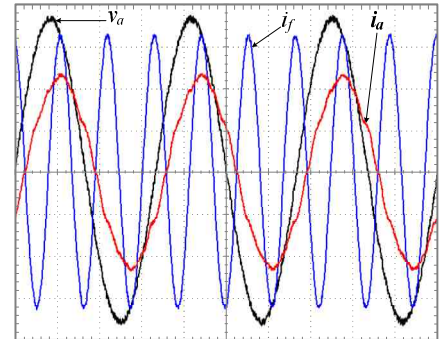Fig. 17. The FFT components of i_a without harmonic injection (0.5A/div).

Fig. 18. The utility line current, i_a and injection current, i_f along with v_a, with optimum harmonic injection current for α=30° (100V/div., and 1A/div.).

The relation between the optimum values of ϕ, ψ and the firing angle, α, of the three-phase converter can be obtained from (5), (6) and (7), as shown in Fig. 6. In case of an operating range of the firing angle, α, between 0° and 60° in the rectifier mode and between 120° and 170° in the inverter mode, the corresponding optimum values of the firing angle of the single, ψ_{opt}, are between 0° and 180° for the rectifier and inverter modes of operation.

IV. DESIGN OF ZIGZAG TRANSFORMER

The third harmonic injection can be transferred to the line current using a zig-zag transformer [16], [20], [22], [23], and, [30]-[32] or a three-phase transformer with an open delta [18], [19]. The required kVA rating of the three-phase transformer with an open delta is $\sqrt{3}$ times the kVA required for a

zig-zag transformer [23]. For this reason a zig-zag transformer has been used in this study. The rms values of the winding voltages are $V_{LL}/3$ [23]. The VA rating of the zig-zag transformer can be obtained from (22), and as discussed before I_{f3}=0.606pu. The VA rating of the zigzag transformer is $S_{zig-zag}$=0.606/3=0.202pu, which means that the VA rating of the zig-zag transformer is about 20.2% of the VA rating of the controlled converter.

$$S_{zig-zag} = V_{ph-zig-zag} * I_f \qquad (22)$$

V. SIMULATION AND EXPERIMENT RESULTS

A prototype model has been introduced to demonstrate the above analysis. The prototype model is designed to feed 2kVA loads with a supply line voltage of 220V. The prototype model is used in simulation and experimental work. The simulation of the proposed technique was performed using the PSIM computer program. Same of the values of the components used in the simulation program have been used in the experimental prototype to compare the results. The simulation and experimental work was performed in the rectifier and inverter modes of operation. The simulation and experimental results are identical and agree with the mathematical analysis. Fig. 12 shows the relation between the THD and the value of q for the mathematical analysis (22) and the experimental analysis at α=20°. This figure reveals that the optimal value of q is 1.5 for the minimum THD as previously concluded from (15). In addition, this figure shows the importance of the third harmonic injection technique in reducing the harmonic contents in utility line currents. The simulation and experimental waveforms for α=20° and 40°, as an example, are shown in the following sections.

A. Experimental results at α=20o

Fig. 13 shows the waveforms of the voltages v_d, v_f and v_{on} at α =20°. Fig. 14 shows the voltages v_d, v_f and v_{on} at α =140°. Fig. 15 and Fig. 16 show the supply current waveforms with respect to the phase a voltage without an injection of the 3rd harmonic current at α =20° as an example of the rectifier and α =140° and as an example of inverter, respectively. Fig. 17 shows the FFT components of i_a without the harmonic injection. It is clear from this figure that the supply current has a very high THD and that it is mostly of 5th and 7th harmonics. The THD of this current is about 54%, which is greater than all of the harmonic standards.

Fig. 18 and Fig. 19 show the utility line current, i_a, the injection current, i_f, and v_a, with the optimum harmonic injection current for α=30° and the FFT components of i_a, respectively. Fig. 20 and Fig. 21 show the utility line current, i_a, the injection current, i_f, and v_a, with the optimum harmonic

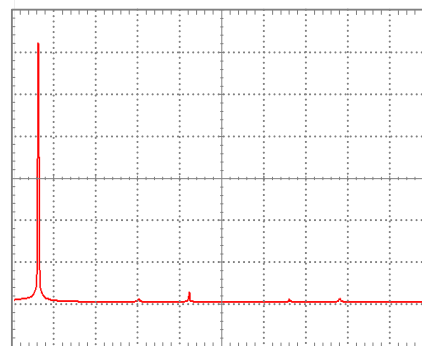
Fig. 19. The FFT components of i_a with optimum harmonic injection current for α=30° (0.5A/div, 100Hz/div.).
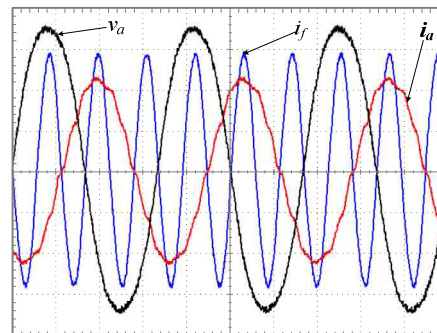

Fig. 20. The utility line current, i_a and injection current, i_f along with v_a, with optimum harmonic injection current for α=130° (100V/div., and 1A/div).
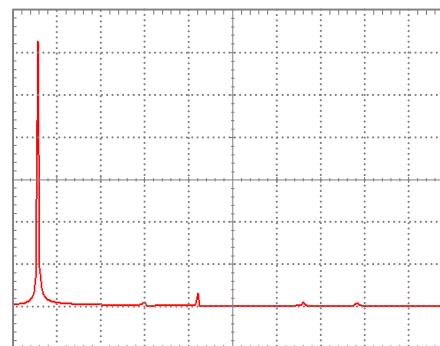

Fig. 21. The FFT components of i_a with optimum harmonic injection current for α=130° (0.5A/div, 100Hz/div.).

injection current for α=130° and the FFT components of i_a, respectively. It is clear from Fig. 19 and Fig. 21 that the THDs are 5.085% and 5.103%, respectively, which is acceptable by harmonic injection standards. The results shown in Fig. 18 to Fig. 21 prove the superiority of the proposed injection technique.

VI. CONCLUSIONS

The utility line currents of three-phase controlled converters have a THD that is higher than the harmonic standard limits. This high THD can produce a lot of problems in power systems. One of the most effective techniques to

deal with this is the circulation of the third harmonic current from the dc-link to the line currents. This paper introduces a single-phase PWM converter in the injection path to control the angle of the injection current for each firing angle of a three-phase controlled converter. The power circulated in the third harmonic injection path is recovered by circulating the power back from the output of the single-phase PWM converter to the dc-link of the three-phase controlled converter. The modulation index and power angle of the single-phase PWM converter can control the amplitude and angle of the 3rd harmonic injection current. In this paper, the optimum relation between the firing angle of the three-phase controlled converter and the power angle of single-phase PWM converter for the minimum THD is introduced. In addition, the optimum amplitude of the injected current is introduced both mathematically and experimentally. The THD of the utility line current from the simulation and experimental results proves the mathematical results for this technique. The THD of the utility line current with the optimal harmonic injection current is about 5% which is lower than limits of harmonics standards.

ACKNOWLEDGMENT

REFERENCES

[1] S.C. Bera, R. Sarkar, N. Mandal, "An opto-isolator based linearization technique of a typical thyristor driven pump Original Research Article," *ISA Transactions*, Vol. 51, No. 1, pp. 220-228, Jan. 2012.

[2] S.C. Bera, N. Mandal, R. Sarkar "A novel technique of using a thyristor driven pump as the final control element and flow indicator of a flow control loop Original Research Article," *ISA Transactions*, Vol. 50, No. 3, pp. 496-503, Jul. 2011.

[3] D. Banerjee and V. T. Ranganathan, "Load-Commutated SCR Current-Source-Inverter-Fed Induction Motor Drive With Sinusoidal Motor Voltage and Current," *IEEE Trans. Power Electron.*, Vol. 24, No. 4, PP. 1048-1061, Apr. 2009.

[4] B. Wu, Multipulse SCR Rectifiers, in High-Power Converters and ac Drives, John Wiley & Sons, Inc., Hoboken, NJ, USA. doi: 10.1002/9780471773719.ch4, 2005.

[5] A. H. Hoevenaars, I. C. Evans, and B. Desai, "Preventing AC drive failures due to commutation notches on a drilling rig," *Record of Conference Petroleum and Chemical Industry Conference*, PP. 1-6, 2009.

[6] D. Habibinia, R. Ghandehari, Y. Najafi, M. Rahimzadeh, H. Khalilpoor, "Study of inverter and rectifier substations islanding fault in HVDC system, and comparison between different control-protective methods," *International Symposium on Power Electronics Electrical Drives Automation and Motion (SPEEDAM)*, pp. 1622-1627, 2010.

[7] B. Jun-Feng, X. Jia-Zhu, and L. Long-Fu, "Characteristics of power transmission and dynamic recovery of FCC-HVDC with different SCR," *International Conference on Power System Technology (POWERCON)*, pp. 1-6, 2010.

[8] Z. Chen, "Compensation Schemes for a SCR Converter in Variable Speed Wind Power Systems," *IEEE Trans. Power Del.*, Vol. 19, No. 2, pp. 813-821, Apr. 2004.

[9] H. Akagi and R. Kondo, "A transformerless hybrid active filter using a three-level pulsewidth modulation (pwm) converter for a medium-voltage motor drive," *IEEE Trans. Power Electron.*, pp. 1365-1374, Vol. 25, No. 6, Jun. 2010.

[10] A. Sarwar and M.S.J. Asghar, "Multilevel converter topology for solar PV based grid-tie inverters," *IEEE International on Energy Conference and Exhibition (EnergyCon),* pp. 501-506, 2010.

[11] S. Yang, F. Meng, and W. Yang; "Optimum design of interphase reactor with double-tap changer applied to multipulse diode rectifier," *IEEE Trans. Ind. Electron.*, Vol. 57, No.9, pp. 3022-3029, Sep. 2010.

[12] A. Bhattacharya and C. Chakraborty, "A shunt active power filter with enhanced performance using ann-based predictive and adaptive controllers," *IEEE Trans. Ind. Electron.*, Vol. 58, No.2, pp. 421-428, Feb. 2011.

[13] A. Luo, X. Xu, L. Fang, H. Fang, J. Wu, and C. Wu "Feedback-feedforward pi-type iterative learning control strategy for hybrid active power filter with injection circuit," *IEEE Trans. Ind. Electron.*, Vol. 57, No. 11, pp. 3767-3779, Nov. 2010.

[14] S. Rahmani, N. Mendalek, and K. Al-Haddad, "Experimental design of a nonlinear control technique for three-phase shunt active power filter," *IEEE Trans. Ind. Electron.* Vol. 57, No.10, pp. 3364-3375, Oct. 2010.

[15] A. M. Eltamaly, "Harmonics reduction of three-phase boost rectifier by modulating duty ratio," *Electric Power Systems Research*, Vol. 77, pp. 1425–1431, Aug. 2007.

[16] P. Pejovic and D. Shmilovitz, "Low-harmonic thyristor rectifiers applying current injection," *IEEE Trans. Aerosp. Electron. Syst.*, Vol.39 No. 4, pp. 1365-1374, Oct. 2003.

[17] Y.H. Liu, J. Arrilaga, N. R. Watson, and L. B. Perera, "Application of the DC-ripple reinjection concept to forced-commutated conversion," *Proc. of IEEE Power Engineering Conf.*, pp. 1-6, 2005.

[18] B. M. Saied and H. I. Zynal, "Harmonic current reduction of a six-pulse thyristor converter," *Proc. of IEEE Electrical Machines and Power Electronics conf.*, pp.596-602, Sep. 2007.

[19] A. Maswood, "Optimal harmonic injection in thyristor rectifier for power factor correction," *IEE Proceedings on Electric Power Applications*, Vol. 150 No. 5, pp. 615-622, Sep. 2003.

[20] A. M. El-Tamaly, P. N. Enjeti, and H. H. El-Tamaly, "An improved approach to reduce harmonics in the utility interface of wind, photovoltaic and fuel cell power systems," *Proc. of IEEE Applied Power Electronics Conference and Exposition, APEC 2000,* Vol. 2, pp. 1059-1065, 2000.

[21] B.M. Saied and H.I. Zynal, "Minimizing current distortion of a three-phase bridge rectifier based on line injection technique," *IEEE Trans. Power Electron.*, Vol. 21, No. 6, pp. 1754-1761, Nov. 2006.

[22] P. Bozovic, P. Pejovic, "Current-injection-based 12-pulse rectifier using a single three-phase diode bridge," *IET Electric Power Applications,* Vol. 1, No. 2, pp. 209-216, Mar. 2007.

[23] P. Pejović, *Three-phase diode rectifiers with Low Harmonics*, Power electronics and power systems, Springer, 2007.

[24] B. Singh, B. N. Singh, A. Chandra, K. Al-Haddad, A. Pandey, and D. P. Kothari, "A review of three-phase improved power quality AC–DC converters," *IEEE Trans. Ind. Electron.*, Vol. 51, No. 3, pp.641-660, Jun. 2004.

[25] B. M. Bird, J. F. Marsh, and P. R. Mclellan, "Harmonic reduction in multiplex converters by triple frequency current injection," *Proc. of the Institution of Electrical Engineers,* Vol. 116, No. 10, Oct. 1969.

[26] B. M. Saied and R. Kh. Antar, "Harmonic mitigation technique for the power quality improvement of DC motor drives," *International Aegean Conference on Electrical Machines and Power Electronics, 2007. ACEMP '07*, pp. 592-595, Sep. 2007.

[27] W. Mielczarski, W. B. Lawrance, R. Nowacki, and D. Grahame Holmes, "Harmonic current reduction in three-phase bridge-rectifier circuits using controlled current injection," *IEEE Trans. Ind. Electron.*, Vol. 44, No. 5, pp. 604-611, Oct. 1997.

[28] M. Villablanca and J. Arrillaga, "Single-bridge unit-connected HVDC generation with increased pulse number," *IEEE Trans. Power Del.*, Vol. 8, No. 2, pp.681-688, Apr. 1993.

[29] J. Boys and B. Mitchell, "Current-forced neutral injection in a three-phase rectifier/converter," *IEE Proceedings Electric Power Applications,* Vol. 146, No. 4, pp. 441-446, Jul. 1999.

[30] P. Bozovic and P. Pejovic, "A novel three-phase full bridge thyristor rectifier based on the controlled third harmonic current injection," *Power Tech Conference Proceedings*, Vol. 1, 2003.

[31] A. M. Eltamaly "A modified harmonics reduction technique for a three-phase controlled converter," *IEEE Trans. Ind. Electron.*, Vol. 55, No. 3, pp.1190-1197, Feb. 2008.

[32] A. M. Eltamaly, *Renewable Energy*, Intechweb publisher, Renewable Energy, ISBN 978-953-7619-52-7, Dec. 2009.

[33] P. Pejovic, "Two three-phase high power factor rectifiers that apply the third harmonic current injection and passive resistance emulation," *IEEE Trans. Power Electron.*, Vol. 15, No. 6, pp.1228-1240, Nov. 2000.

Ali M. Eltamaly was born in Egypt, in 1969. He received his B.S. (with Distinction and Honors) and M.S., in 1992 and 1996, respectively, and his Ph.D. from the Department of Electrical and Computer Engineering, Texas A&M University, USA, in 2000. He was a faculty member in the College of Engineering, Minia University, Minya, Egypt, and in the College of Engineering, Mansoura Universities, Mansoura, Egypt, from 1993 to 2005. He has been a member of the Sustainable Energy Technology Center, Department of Electrical Engineering, King Saud University, Riyadh, Saudi Arabia, since October 2005. His current research interests include power electronics, motor drives, power quality and renewable energy. He has supervised a number of M.S. and PhD theses, worked on number of technical projects and published three books and more than 55 papers in these areas. He has joined the editorial board of some scientific journals as well as the steering committees of many international conferences.